

The orientation of spheroidal microorganisms swimming in a flow field

By T. J. PEDLEY¹ AND J. O. KESSLER²

¹ Department of Applied Mathematics and Theoretical Physics,

University of Cambridge, Silver Street, Cambridge CB3 9EW, U.K.

² Department of Physics, University of Arizona, Tucson, Arizona 85721, U.S.A.

(Communicated by Sir James Lighthill, F.R.S. – Received 15 September 1986)

This paper shows how to calculate local equilibrium orientations of inhomogeneous spheroidal particles placed in a flow field. The results can be applied either to dilute suspensions of inert particles or to swimming microorganisms; illustrative examples are chosen with the latter application in mind. The centre of mass of a particle is displaced from the geometric centre C along the axis of symmetry, and the orientation of this axis (represented by the unit vector \mathbf{p}) is determined from the balance between the gravitational couple, non-zero when \mathbf{p} is not vertical, and the viscous couple exerted by the surrounding fluid. Fluid and particle inertia are neglected. ‘Local equilibrium’ means that \mathbf{p} is stationary in a suitable frame of reference, which may be the laboratory frame or one rotating rigidly relative to it, at the values of fluid velocity, vorticity and rate of strain evaluated at C in the absence of the particle. It is also shown how to determine the stability of local equilibria. Stable equilibrium values of \mathbf{p} are calculated explicitly for a number of experimentally realizable flow fields, including vertical Poiseuille flow in a pipe, conical sink flow, two-dimensional straining and shearing flows in a vertical plane, and the wake of a falling sphere. The analysis is particularly simple for spherical particles, when the local rate of strain does not contribute to the viscous couple. The results have implications for laboratory manipulation of the trajectories of swimming algae, and for the development of collective behaviour and the existence of critical phenomena in suspensions of them.

1. INTRODUCTION

The balance of viscous and gravitational torques which act on microorganisms can determine their orientation. Since the orientation of a swimming cell directs its trajectory, this torque balance results in directed locomotion, called gyrotaxis (Kessler 1984, 1985a, b, 1986a, b). Gyrotaxis affects pattern formation in laboratory suspensions of swimming algae. It can also be used to concentrate these motile cells and to separate polydisperse populations. The previous treatments of gyrotaxis have only dealt with spherical cells in simple ambient flows. This paper extends the theory to predict the orientation of spheroidal cells in general flows. It explicitly ignores orienting mechanisms controlled by the microorganisms themselves, or by collisions among them. The swimmers are considered as automata with invariant morphology, swimming speed, and a propulsion direction

that is fixed in relation to an internal axis of symmetry. Although real cells exhibit stochastic behaviour, the predictive success of the theory describing gyrotaxis of spherical swimmers implies that a deterministic theory provides a useful description of the actual mean behaviour of the organisms. Thus the results obtained here should be thought of as predicting peaks in the distributions of orientation of actual cells.

A typical algal cell considered here, such as *Chlamydomonas* or *Dunaliella*, has approximately the shape of a prolate spheroid with a pair of flagella at one end by which the cell swims in a direction roughly parallel to its axis. The centre of mass of the cell, however, is displaced away from the geometrical centre, towards the back. Thus the cells are bottom-heavy, and naturally tend to swim vertically upwards in a fluid otherwise at rest; if they started to swim at an angle to the vertical, the gravitational couple would immediately rotate them to the vertical. However, if the fluid medium flows with a horizontal component of vorticity, it will exert a viscous torque on the cell and rotate it away from the vertical. If the vorticity is not too large, a balance will be struck between the viscous and gravitational torques, and the cell will swim at a fixed angle θ to the vertical (see figure 1). This is the mechanism of gyrotaxis of spherical cells. Kessler showed that θ is given by

$$\sin \theta = B\omega, \quad (1)$$

where ω is the horizontal component of vorticity in the flow, and B is a constant with the dimension of time (defined in equation (11) below) that is determined by the mass and geometry of the cell and the viscosity of the suspending fluid. We may note that no equilibrium is possible, and the cell will tumble, if ω exceeds the critical value B^{-1} (Kessler 1986a).

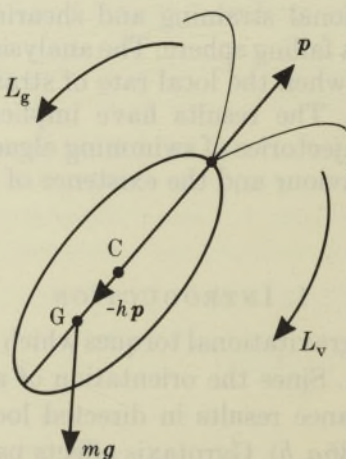


FIGURE 1. The torque balance on a cell.

Gyrotaxis can be demonstrated by the accumulative behaviour of swimming algae suspended in a vertical cylindrical Poiseuille flow. When the flow is directed downwards, the cells swim towards its axis, forming a concentrated focused beam (figure 2a). When the flow is upwards, the sign of $\sin \theta$ reverses and the cells swim towards its periphery. This phenomenon can be used to separate populations of

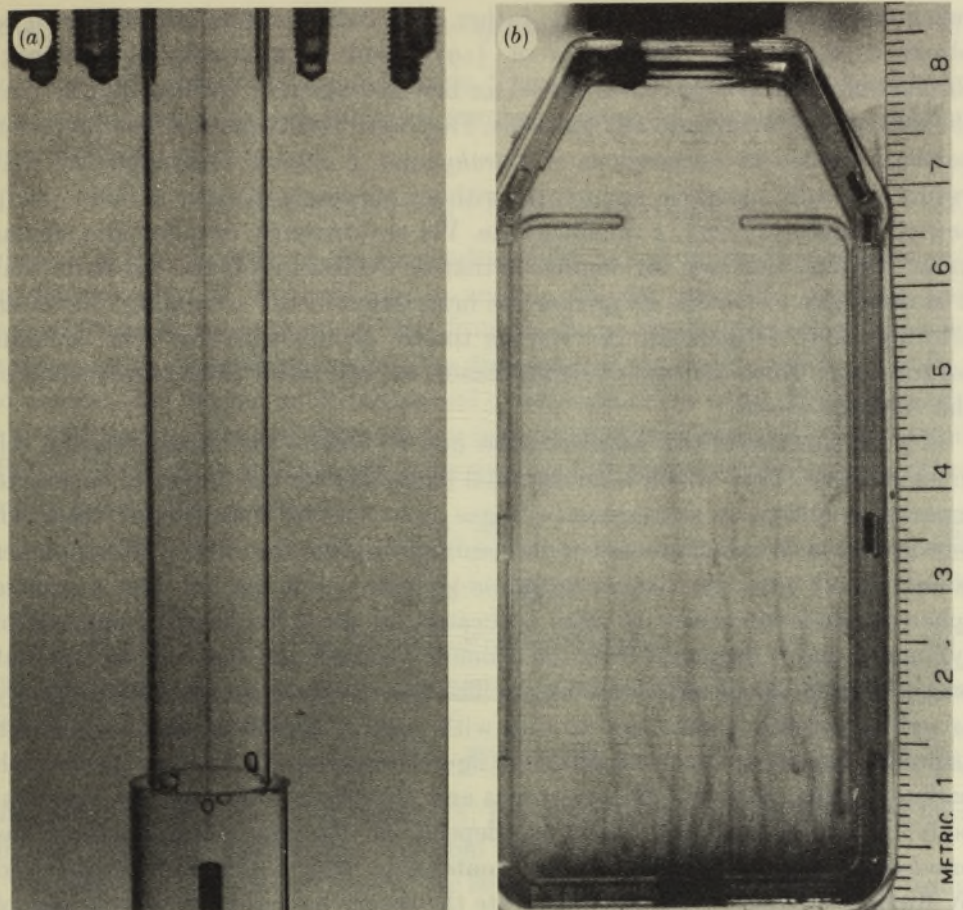


FIGURE 2(a). Hydrodynamically focused beam of *Chlamydomonas nivalis*. The photograph shows an aqueous medium containing cells which were originally uniformly dispersed, above the level of the picture, flowing downward in a round cylindrical cavity. At the level shown, the cells have swum towards the axis where they appear as a streak which absorbs and scatters diffuse light incident from the rear of the perspex apparatus. The internal diameter of the cylinder is 1.2 cm; the fluid velocity is approximately 0.1 cm s^{-1} on the axis. (b) Self-generated plumes of gyrotactic cells. A culture of *C. nivalis* containing $5 \times 10^5 \text{ cells cm}^{-3}$ has developed self-concentrated descending plumes separated by ascending regions of fluid with low cell concentration. The concentrated regions sink because the cell density is about 5% greater than that of water. The velocity profile of the sinking regions concentrates cells by the same mechanism as shown in figure (a). The vessel shown is 2 cm deep and filled to the cap; the cell culture was uniformly mixed 5 min before the photograph was taken.

cells with diverse properties into subpopulations of lesser diversity, e.g. rapid swimmers from slow ones. To realize the full potential of such 'gyrotactic separation' procedures in the laboratory, a thorough understanding of the mechanics of cell-body orientation is essential.

The cells under discussion are slightly denser than water, usually by about 5%. Thus when they are suspended in a layer of fluid at rest, and swim upwards, they cause the upper levels of that fluid to become denser than the lower levels, so that an overturning convection takes place. This phenomenon, now known as bioconvection, has been familiar for a number of years (Nultsch & Hoff (1973) and

references therein; Childress 1981); rather dense falling sheets or plumes can be observed (figure 2b). Childress *et al.* (1975) and Levandowsky *et al.* (1975) formulated a theoretical, linear model for bioconvection, on the assumption that the cells always swim generally upwards. They were able to predict the convection patterns formed by suspensions of *Tetrahymena*, a ciliated microorganism that swims vertically upwards, apparently without gyrotaxis (Kessler & Cann 1987), and of *Cryptocodinium*, a dinoflagellate. We are currently developing a similar model for bioconvection for organisms that do exhibit gyrotaxis, but to do that it is necessary to be able to predict the orientation of the swimming cells in an arbitrary flow. In general, the viscous torque on non-spherical cells contains contributions from the rate-of-strain tensor, as well as all three components of the vorticity vector.

It is the purpose of this paper to show how to predict the orientation of a cell in an arbitrary flow, which is an essential ingredient for the design of devices to separate polydisperse suspensions of algae as well as for a continuum theory of bioconvection. We shall proceed on the assumptions that the cell Reynolds number is very small, that the viscous torque is the same as if the cell were a prolate spheroid, that the centre of mass is located on the cell's longitudinal axis of symmetry and is displaced from the geometric centre, and that the flagella that propel the cell do not affect the torque. The theory can be applied to nose-heavy as well as tail-heavy cells, and to cells with pushing flagella at the back as well as pulling flagella at the front, although figure 1 is drawn for tail-heavy cells with pulling flagella, such as *Chlamydomonas* and *Dunaliella*. The case of a spherical body, in which the torque does not depend on the rate-of-strain tensor, has previously been solved (in a different context) by Hall & Busenberg (1969) and by Brenner (1970*a, b*). We shall illustrate the theory by a number of examples of different types of flow, many of which can be realized experimentally. In many cases more than one local equilibrium orientation appears to be possible, but several of them can often be ruled out because they are unstable. Thus in each example we shall (a) predict the local equilibrium orientations, (b) test them for stability and (c) predict conditions in which a steady orientation cannot be achieved and the cells are expected to tumble, such as $\omega > B^{-1}$ in the case given by equation (1).

2. GENERAL FORMULATION

2.1. Swimming direction

Suppose that the cell is a prolate spheroid with mass m , volume v , semi-major axis a and semi-minor axis b , and that its major axis contains the unit vector \mathbf{p} (figure 1) which points along the direction of the cell's propulsion. The centre of mass is displaced a distance h from the geometric centre, C , to position $-h\mathbf{p}$ relative to C . The sign is chosen to correspond with the geometry of the algal cells previously considered by Kessler (1984, 1985*a, b*, 1986*a, b*, 1987); for nose-heavy cells the sign reverses. In the absence of inertia it is necessary that the total couple \mathbf{L} on the cell, i.e. the sum of the gravitational couple \mathbf{L}_g and the viscous torque \mathbf{L}_v , be zero:

$$\mathbf{L} = \mathbf{L}_g + \mathbf{L}_v = 0. \quad (2)$$

Now $L_g = -hp \wedge mg$, (3)

where \mathbf{g} is the gravitational acceleration. The viscous torque on an isolated body in a general flow with zero Reynolds number is given by the following equation from Rallison (1978):

$$L_{vi} = -\mu v [P_{ij}(v_j - u_j) + Y_{ij}(\Omega_j - \frac{1}{2}\omega_j) + R_{ijk} e_{jk}], \quad (4)$$

where μ is the viscosity of the suspending fluid; \mathbf{v} and $\boldsymbol{\Omega}$ are the velocity and angular velocity of the body; \mathbf{u} , $\boldsymbol{\omega}$ and e_{ij} are the velocity, vorticity and rate-of-strain tensor in the fluid 'far' from the body (the length scale of the flow is supposed to be much larger than the dimension of the body); and P_{ij} , Y_{ij} , R_{ijk} are tensors that depend on the shape and orientation of the body. When the body is a rigid prolate spheroid these tensors take the following relatively simple form (Batchelor 1970), in which \mathbf{q} and \mathbf{r} are unit vectors perpendicular to each other and to \mathbf{p} , such that $\mathbf{q} \wedge \mathbf{r} = \mathbf{p}$:

$$P_{ij} = 0, \quad (5)$$

$$Y_{ij} = \alpha_{\parallel} p_i p_j + \alpha_{\perp} (q_i q_j + r_i r_j), \quad (6)$$

$$R_{ijk} = -\alpha_0 Y_{il} (r_l p_j q_k - q_l p_k r_j). \quad (7)$$

The quantities α_0 , α_{\parallel} and α_{\perp} are dimensionless constants; α_0 measures the eccentricity of the spheroid,

$$\alpha_0 = (a^2 - b^2)/(a^2 + b^2), \quad (8)$$

and α_{\parallel} and α_{\perp} are given in the Appendix. The object of this section is to show how to find local equilibrium values of \mathbf{p} from the above equations.

Because e_{ij} is a symmetric tensor, the last term in (4) can be simplified, by using (7), to

$$R_{ijk} e_{jk} = -\alpha_0 Y_{il} \epsilon_{klm} p_m p_j e_{jk}. \quad (9)$$

If we now let \mathbf{k} be a unit vector directed vertically upwards, so that $\mathbf{g} = -g\mathbf{k}$, we can combine equations (2)–(7) and (9) to give

$$-[(\alpha_{\parallel}/\alpha_{\perp}) p_i p_l + q_i q_l + r_i r_l] [2\Omega_l - \omega_l - 2\alpha_0 \epsilon_{klm} p_m p_j e_{jk}] + B^{-1} \epsilon_{ijk} p_j k_k = \tilde{L}_i = 0, \quad (10)$$

where

$$B = \mu \alpha_{\perp} / 2h\rho g \quad \text{and} \quad \tilde{L} = 2L / \mu v \alpha_{\perp}, \quad (11)$$

where $\rho = m/v$ is the cell's density, ca. 1.05 g cm⁻³. Note that B has the dimensions of time; when $h \approx 0.1$ μm (Kessler 1986b), $B \approx \alpha_{\perp}/2$ or about 1 s.

It is necessary now to specify both what we mean by 'local equilibrium' and what direction will be taken by the cell's angular velocity $\boldsymbol{\Omega}$. The centre, C, of the cell will move with a velocity equal to the vector sum of the fluid velocity \mathbf{u} and the swimming velocity $V_c \mathbf{p}$. By local equilibrium we mean that $d\mathbf{p}/dt = 0$ in some frame of reference in which C is at rest, at the local instantaneous values of \mathbf{u} , $\boldsymbol{\omega}$, e_{ij} . In our analysis this frame, which will in general have an angular velocity, $\boldsymbol{\Omega}_c$, is explicitly chosen to simplify the problem by taking account of the symmetry of the flow field. In terms of Cartesian axes, it is natural to choose a frame with one axis (say the 3-axis) vertical and another (the 1-axis) horizontal, through C (see figure 3); $\boldsymbol{\Omega}_c$ is then a vertical vector. If the flow is two-dimensional in a vertical

plane, so that \mathbf{u} lies in the same vertical plane as \mathbf{p} and \mathbf{q} , the frame is the inertial, laboratory frame, and $\boldsymbol{\Omega}_c = 0$. On the other hand, for axisymmetric flow with swirl about a vertical axis, this axis of symmetry will be the 3-axis, and $\boldsymbol{\Omega}_c$ will be non-zero, equal in magnitude to the azimuthal (2-) component of the velocity of C divided by the radial distance of C from this axis. The equilibrium is termed 'local', because both the motion of the fluid and the swimming of the cell will cause C to move to points with different values of \mathbf{u} , $\boldsymbol{\omega}$, and e_{ij} ; in such a motion $\boldsymbol{\Omega}_c$ might also change.

The variation of \mathbf{p} with time is in general given by

$$\frac{d\mathbf{p}}{dt}|_{\text{inertial frame}} = \frac{d\mathbf{p}}{dt}|_{\text{rotating frame}} + \boldsymbol{\Omega}_c \times \mathbf{p} = \boldsymbol{\Omega} \times \mathbf{p}, \quad (12)$$

so, in equilibrium, $(\boldsymbol{\Omega} - \boldsymbol{\Omega}_c) \times \mathbf{p} = 0$, or

$$\boldsymbol{\Omega} - \boldsymbol{\Omega}_c = \boldsymbol{\Omega}' \mathbf{p} \quad (13)$$

for some $\boldsymbol{\Omega}'$; $\boldsymbol{\Omega} = \boldsymbol{\Omega}' \mathbf{p}$ only when $\boldsymbol{\Omega}_c = 0$. We now define

$$\boldsymbol{\omega}' = \boldsymbol{\omega} - 2\boldsymbol{\Omega}_c, \quad (14)$$

a known vector, so that the term $2\boldsymbol{\Omega}_l - \boldsymbol{\omega}_l$ in (10) becomes $2\boldsymbol{\Omega}' p_l - \boldsymbol{\omega}'_l$.

We should note further that the viscous torque \mathbf{L}_v does not include a contribution from any active swimming motions that the cell may make. It is often observed (see, for example, Rüffer & Nultsch 1985; Nultsch 1983) that in a still fluid, the flagella cause the cell to rotate; they do so by exerting a torque, which is exactly balanced by a viscous resistive torque, so the net total is zero and does not contribute to the torque balance (2). Of course, if the self-generated angular velocity $\boldsymbol{\Omega}_s$ were not parallel to \mathbf{p} , no local equilibrium value of \mathbf{p} could exist (although there is an equilibrium value of the axis of the cone on which \mathbf{p} lies). If $\boldsymbol{\Omega}_s$ is parallel to \mathbf{p} it will be superimposed on the purely passive angular velocity $\boldsymbol{\Omega}' \mathbf{p}$ (equation (13)) that the body acquires from the surrounding fluid; however, in the rest of this paper we shall ignore $\boldsymbol{\Omega}_s$.

The precise specification of the coordinate system is made as follows. We take the 3-axis vertically upwards (parallel to \mathbf{k}) but not passing through the cell centre C, and the 1-axis horizontal in the plane of \mathbf{k} and C (figure 3). Thus all components of $\boldsymbol{\omega}'_i$ and e_{jk} are given. Taking the scalar product of (10) with \mathbf{p} , \mathbf{q} , \mathbf{r} , in turn, we obtain

$$\tilde{\mathbf{L}} \cdot \mathbf{p} = (\alpha_{\parallel}/\alpha_{\perp})(\boldsymbol{\omega}' \cdot \mathbf{p} - 2\boldsymbol{\Omega}') = 0 \quad (15)$$

$$\tilde{\mathbf{L}} \cdot \mathbf{q} = \boldsymbol{\omega}' \cdot \mathbf{q} - B^{-1} r_3 - 2\alpha_0 p_j r_k e_{jk} = 0 \quad (16)$$

$$\tilde{\mathbf{L}} \cdot \mathbf{r} = \boldsymbol{\omega}' \cdot \mathbf{r} + B^{-1} q_3 + 2\alpha_0 p_j q_k e_{jk} = 0. \quad (17)$$

The first of these identifies the relative angular velocity $\boldsymbol{\Omega}'$ with the component of $\frac{1}{2}\boldsymbol{\omega}'$ parallel to \mathbf{p} .

It is in general less convenient to work with Cartesian coordinates than with the Euler angles θ, ϕ ($0 \leq \theta \leq \pi; -\pi < \phi \leq \pi$; figure 3): θ is the angle \mathbf{p} makes with the vertical, and ϕ is the angle between the vertical plane containing \mathbf{p} and the 1-3 plane. Moreover we choose \mathbf{q} to lie in the vertical plane containing \mathbf{p} , and \mathbf{r}

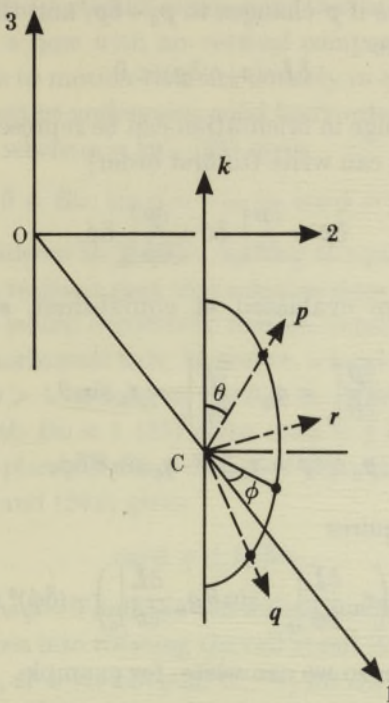


FIGURE 3. Axes and Euler angles.

is therefore horizontal, perpendicular to that plane (thus q and r are not fixed in the body). Hence the (1, 2, 3) components of p , q , r are

$$\left. \begin{aligned} p &= (\sin \theta \cos \phi, \sin \theta \sin \phi, \cos \theta) \\ q &= (\cos \theta \cos \phi, \cos \theta \sin \phi, -\sin \theta) \\ r &= (-\sin \phi, \cos \phi, 0). \end{aligned} \right\} \quad (18)$$

Inserting these into (17) and (16) we obtain the following equations:

$$\begin{aligned} \tilde{L}_\theta \equiv \tilde{L} \cdot r &= -B^{-1} \sin \theta + \omega'_2 \cos \phi - \omega'_1 \sin \phi \\ &+ \alpha_0 \{ \sin 2\theta (e_{11} \cos^2 \phi + 2e_{12} \sin \phi \cos \phi + e_{22} \sin^2 \phi - e_{33}) \\ &+ 2 \cos 2\theta (e_{13} \cos \phi + e_{23} \sin \phi) \} = 0; \end{aligned} \quad (19)$$

$$\begin{aligned} \tilde{L}_\phi / \sin \theta \equiv -\tilde{L} \cdot q &= -\omega'_1 \cos \theta \cos \phi - \omega'_2 \cos \theta \sin \phi + \omega'_3 \sin \theta \\ &+ \alpha_0 \{ \sin \theta (-e_{11} \sin 2\phi + 2e_{12} \cos 2\phi + e_{22} \sin 2\phi) \\ &+ 2 \cos \theta (-e_{13} \sin \phi + e_{23} \cos \phi) \} = 0. \end{aligned} \quad (20)$$

$\tilde{L} \cdot q$ is multiplied by $(-\sin \theta)$ in the definition of \tilde{L}_ϕ for convenience in the subsequent stability analysis. In the examples examined in §3, equations (19) and (20) are solved for θ and ϕ .

2.2. Stability

The equilibrium orientation, in which $(p, q, r) = (p_0, q_0, r_0)$, say, will be stable if a small perturbation in orientation leads to a couple that tends to reduce the

perturbation to zero. Thus if \mathbf{p} changes to $\mathbf{p}_0 + \delta\mathbf{p}$, and the couple changes from zero to $\delta\mathbf{L}$, then we require

$$\delta\mathbf{L} \cdot (\mathbf{p}_0 \wedge \delta\mathbf{p}) < 0 \quad (21)$$

for stability. Now the change in orientation can be represented by changes $\delta\theta, \delta\phi$ in the angles θ, ϕ , and we can write (to first order)

$$\delta\mathbf{p} = \frac{\partial \mathbf{p}}{\partial \theta} \Big|_0 \delta\theta + \frac{\partial \mathbf{p}}{\partial \phi} \Big|_0 \delta\phi,$$

where the derivatives are evaluated at equilibrium, and there is a similar expression for $\delta\mathbf{L}$. But

$$\frac{\partial \mathbf{p}}{\partial \theta} \Big|_0 = \mathbf{q}_0, \quad \frac{\partial \mathbf{p}}{\partial \phi} \Big|_0 = \mathbf{r}_0 \sin \theta,$$

so

$$\mathbf{p}_0 \wedge \delta\mathbf{p} = \mathbf{r}_0 \delta\theta - \mathbf{q}_0 \sin \theta \delta\phi,$$

and the condition (21) requires

$$(\delta\theta)^2 \mathbf{r}_0 \cdot \frac{\partial \tilde{\mathbf{L}}}{\partial \theta} \Big|_0 + \delta\theta \delta\phi \left(\mathbf{r}_0 \cdot \frac{\partial \tilde{\mathbf{L}}}{\partial \phi} \Big|_0 - \sin \theta \mathbf{q}_0 \cdot \frac{\partial \tilde{\mathbf{L}}}{\partial \theta} \Big|_0 \right) - (\delta\phi)^2 \sin \theta \mathbf{q}_0 \cdot \frac{\partial \tilde{\mathbf{L}}}{\partial \phi} \Big|_0 < 0. \quad (22)$$

Now $\tilde{\mathbf{L}} = 0$ at equilibrium, so we can write, for example,

$$\mathbf{r}_0 \cdot \frac{\partial \tilde{\mathbf{L}}}{\partial \theta} \Big|_0 = \frac{\partial}{\partial \theta} (\mathbf{r}_0 \cdot \tilde{\mathbf{L}}) \Big|_0 = \frac{\partial \tilde{\mathbf{L}}_\theta}{\partial \theta}$$

and $-\sin \theta \mathbf{q}_0 \cdot \frac{\partial \tilde{\mathbf{L}}}{\partial \theta} \Big|_0 = \frac{\partial}{\partial \theta} (-\sin \theta \mathbf{q}_0 \cdot \mathbf{L}) \Big|_0 = \frac{\partial \tilde{\mathbf{L}}_\phi}{\partial \theta}$, and so on.

The condition for the quadratic expression (22) to be negative for all possible perturbations $\delta\theta, \delta\phi$ then becomes (dropping the suffix zero)

$$\frac{\partial \tilde{\mathbf{L}}_\theta}{\partial \theta} < 0 \quad \text{and} \quad 4 \left(\frac{\partial \tilde{\mathbf{L}}_\theta}{\partial \theta} \right) \left(\frac{\partial \tilde{\mathbf{L}}_\phi}{\partial \phi} \right) > \left(\frac{\partial \tilde{\mathbf{L}}_\theta}{\partial \phi} + \frac{\partial \tilde{\mathbf{L}}_\phi}{\partial \theta} \right)^2. \quad (23a)$$

(This also implies $\partial \tilde{\mathbf{L}}_\phi / \partial \phi < 0$.)

In the special case in which \mathbf{p}_0 is vertical ($\sin \theta = 0$), the stability condition (21) reduces directly to

$$\tilde{\mathbf{L}}_{\delta\theta} \sin \delta\theta < 0 \quad \text{for all } \phi. \quad (23b)$$

3. EXAMPLES

3.1. Spherical cell

In this case $\alpha_0 = 0$, so the rate-of-strain tensor in the fluid exerts no torque on the cell, which responds solely to the vorticity. This is the case considered by Hall & Busenberg (1969) and Brenner (1970*a, b*); we repeat the solution here (briefly) for completeness. Equations (19) and (20) reduce to:

$$-\omega_1 \sin \phi + \omega_2 \cos \phi = B^{-1} \sin \theta; \quad (24a)$$

$$\omega_1 \cos \phi + \omega_2 \sin \phi = \omega'_3 \tan \theta. \quad (24b)$$

(Note that it is only in the vertical 3-component that ω' (equation (14)) can differ from ω .) Consider first a flow with no vertical component of relative vorticity: $\omega'_3 = 0$; this corresponds to motion that lies entirely in a vertical plane relative to axes that are either at rest or undergoing solid body rotation about a vertical axis. In this case, if $B\omega \leq 1$, where $\omega = |\omega'|$, (24) gives

$$\sin \theta = B\omega; \sin \phi = -\omega_1/\omega, \cos \phi = \omega_2/\omega; \quad (25)$$

this is just the case considered by Kessler, leading to equation (1); see also Brenner (1970a). These authors realized that this solution does not exist for $B\omega > 1$ and predicted that the cells would constantly tumble, rotating with variable angular velocity about a fixed horizontal axis. However, a local equilibrium solution does exist for $\omega'_3 = 0$ and $B\omega > 1$, as long as $\tan \theta = \infty$. Without loss of generality let $\omega_1 = 0$, $\omega_2 = \pm \omega$, so with $B\omega < 1$ (25) gives $\cos \phi = \pm 1$, i.e. $\phi = 0$ or π and the cell axis lies in the 1-3 plane. If $B\omega > 1$, and $\theta = \frac{1}{2}\pi$, then the right-hand side of (24b) is indeterminate, and (24a) gives

$$\cos \phi = \pm 1/B\omega. \quad (26)$$

In the limit $B\omega \rightarrow \infty$, $\cos \phi \rightarrow 0$ and the cell axis is in the 2-direction; in this case the viscous torque all goes into rotating the cell about its axis: equation (15) gives $\Omega \approx \frac{1}{2}\omega$. More generally, $\Omega = (1/2B)\sqrt{(\omega^2 B^2 - 1)}$ for $\omega B > 1$ and $\omega'_3 = 0$. Whether the cells tumble or not will depend on whether this equilibrium is stable.

The above results can be derived as limiting cases of the general solution of equations (24) for non-zero ω'_3 , which is as follows:

$$\cos^2 \theta = \frac{1}{2}(1 - B^2\omega^2 + \sqrt{(1 - B^2\omega^2)^2 + 4B^2\omega'^2_3}) \quad (27a)$$

$$\cos \phi = (\omega_1 \omega'_3 \tan \theta + \omega_2 B^{-1} \sin \theta) / (\omega_1^2 + \omega_2^2) \quad (27b)$$

$$\sin \phi = (\omega_2 \omega'_3 \tan \theta - \omega_1 B^{-1} \sin \theta) / (\omega_1^2 + \omega_2^2); \quad (27c)$$

the right-hand side of (27a) lies between 0 and 1 for all non-zero values of $B\omega$ and $B\omega'_3$ ($|\omega'_3| < \omega$). In investigating the stability of this equilibrium, we note that

$$\partial \tilde{L}_\theta / \partial \theta = -B^{-1} \cos \theta,$$

which is negative (necessary for stability) provided $\cos \theta$ is chosen to be the positive square root of (27a); i.e. the cell must be nose-up, as one would intuitively expect. The same criterion ensures that $\partial \tilde{L}_\phi / \partial \phi < 0$, and the second inequality in (23a) is automatically satisfied because the right-hand side is zero. Thus the equilibrium is always stable for non-zero values of ω'_3 (cf. Hall & Busenberg 1969). If ω'_3 is zero, however, the equilibrium with $\cos \theta = 0$ ($B\omega > 1$) is neutrally stable by the criteria in (24) since every term is zero. Taking the stability analysis of §2.2 to higher order, we notice that a sufficient condition for higher-order instability of such a neutrally stable equilibrium is $\partial^2 L_\theta / \partial \theta^2 \neq 0$. In the present case this quantity is equal to $B^{-1} \sin \theta$, which is non-zero when $\cos \theta = 0$.

We therefore confirm that Kessler's conclusions were correct for flows with $\omega'_3 = 0$: stable equilibrium with $\sin \theta = B\omega$ if $B\omega < 1$, so the cells focus inwards in a meridional plane, but no stable equilibrium if $B\omega > 1$, so the cells will tumble. However, when ω'_3 is non-zero the equilibrium is always stable. If we suppose that

ω'_3 is very small, $\omega_1 = 0$, $\omega_2 \approx -\omega$ (< 0 as for downwards Poiseuille flow), we can see that, as ω increases above B^{-1} , there will be a rapid transition from a stable equilibrium with $\sin \theta \approx B\omega$ and $\phi \approx \pi$ to one with $\sin \theta \approx 1$ and $\cos \phi \approx -1/B\omega$. So in this case the cells will not tumble, but will continue to focus inwards, via spiral trajectories. Presumably, of course, if ω'_3 is very small, the equilibrium with $\sin \theta \approx 1$ will be nonlinearly unstable for not very large disturbances.

One might use these results for an investigation of illumination-guided swimming of algae. The steering mechanism of these cells, relative to the direction of an incident light beam, appears to depend on their autorotation (Nultsch 1983). If the cells' rotation rate can be increased, decreased or stopped, their orienting sense, or their ability to respond, would very probably be modified, and thus the effects of rotation would be separated from other steps in their control system. This modification of their rotation rate could be accomplished by a proper choice of ωB and $\omega'_3 B$, which would cause a controlled spin, Ω' , to be added to the angular velocity of autorotation.

3.2. Vertical, axisymmetric flow

We use cylindrical polar coordinates (r, λ, z) , with the origin (figure 3) on the axis of symmetry, which is always taken to be vertical; the Cartesian coordinates $(1, 2, 3)$ defined above are in the (r, λ, z) directions respectively. We assume in general that there is no swirl, and the velocity components are taken to be $[U(r, z), 0, W(r, z)]$, so that the vorticity is entirely in the λ -direction and is given by

$$\omega_1 = \omega'_3 = 0, \quad \omega_2 = \omega = U_z - W_r, \quad (28)$$

where suffices r, z refer to partial differentiation. The components of the rate of strain tensor are

$$\begin{aligned} e_{11} &= U_r, & e_{22} &= U/r, & e_{33} &= W_z, \\ e_{13} &= \frac{1}{2}(U_z + W_r), & e_{12} &= e_{23} &= 0. \end{aligned} \quad (29)$$

(a) Downwards Poiseuille flow

This is the flow in which gyrotactic focusing was originally demonstrated (Kessler 1984). For a pipe of radius a_0 the velocity components are

$$U = 0, \quad W = -W_0(1 - r^2/a_0^2),$$

where W_0 is the peak velocity, so that

$$\omega = -2\sigma, \quad e_{13} = \sigma, \quad \text{where } \sigma = W_0 r/a_0^2, \quad (30)$$

while all other components of e_{ij} are zero. The local equilibrium equations (19) and (20) become:

$$\tilde{L}_\theta = -B^{-1} \sin \theta - 2\sigma \cos \phi (1 - \alpha_0 \cos 2\theta) = 0; \quad (31a)$$

$$\tilde{L}_\phi / \sin \theta = 2\sigma (1 - \alpha_0) \cos \theta \sin \phi = 0. \quad (31b)$$

Since $\alpha_0 < 1$, these equations show that there are two possible equilibria, E 1 and E 2, as follows.

$$\text{E 1. } \cos \theta = 0 \quad \text{so} \quad \theta = \frac{1}{2}\pi, \quad \cos \phi = -1/2B\sigma(1 + \alpha_0); \quad (32)$$

this represents a real orientation as long as

$$2B\sigma(1+\alpha_0) \geq 1. \quad (33)$$

E 2. $\sin \phi = 0$ so $\phi = 0$ or π , $\cos \phi = \pm 1$,

$$\sin \theta = \mp 2B\sigma(1-\alpha_0 \cos 2\theta); \quad (34)$$

in fact the lower sign must be taken (implying $\phi = \pi$) since $\sin \theta \geq 0$ ($0 \leq \theta \leq \pi$). Equation (34) can be solved to give

E 2_±. $\sin \theta = [1 \pm \sqrt{(1 - 32B^2\sigma^2\alpha_0(1-\alpha_0))}] / 8B\sigma\alpha_0.$ (35)

These roots are real (and positive) only if

$$32B^2\sigma^2\alpha_0(1-\alpha_0) \leq 1; \quad (36)$$

when this is satisfied the roots will represent real orientations if they are below 1. Two possibilities arise. Either $8B\sigma\alpha_0 > 1$, in which case the lower sign in (35) (equilibrium E 2₋) always gives $\sin \theta < 1$ and the upper sign (E 2₊) does so if (33) is satisfied too; however, $8B\sigma\alpha_0 > 1$ is inconsistent with (36) unless $\alpha_0 > \frac{1}{3}$, but in that case (33) is satisfied. Or $8B\sigma\alpha_0 < 1$, in which case the upper root of (35) cannot be below 1, and the lower root (E 2₋) is below 1 if $2B\sigma(1+\alpha_0) \leq 1$, whatever the value of α_0 .

These results can be summarized as follows. For all α_0 , if $B\sigma < [2(1+\alpha_0)]^{-1}$ (i.e. (33) is not satisfied) the only possible equilibrium is E 2₋; if $B\sigma > [2(1+\alpha_0)]^{-1}$ then equilibrium E 1 is possible, and for $\alpha_0 < \frac{1}{3}$ that is the only one. However, for $\alpha_0 > \frac{1}{3}$ both E 2₊ and E 2₋ are possible in addition to E 1 if $[2(1+\alpha_0)]^{-1} < B\sigma < [32\alpha_0(1-\alpha_0)]^{-\frac{1}{2}}$. For $\alpha_0 = 0$ these results reduce to those of §3.1 with $\omega'_3 = 0$.

Each of the equilibria E 2_±, when it exists, corresponds to two values of θ , one less and one greater than $\frac{1}{2}\pi$. When E 2₋ exists it is stable for $\theta < \frac{1}{2}\pi$ (nose-up) since, for E 2_±,

$$\frac{\partial \tilde{L}_\theta}{\partial \theta} = \pm B^{-1} \cos \theta \sqrt{[1 - 32B^2\sigma^2\alpha_0(1-\alpha_0)]},$$

$$\frac{\partial \tilde{L}_\phi}{\partial \phi} = -\sigma(1-\alpha_0) \sin 2\theta, \quad \frac{\partial \tilde{L}_\theta}{\partial \phi} + \frac{\partial \tilde{L}_\phi}{\partial \theta} = 0;$$

on the other hand E 2₊ is always unstable. Moreover, E 1 is always unstable too, since

$$\frac{\partial \tilde{L}_\theta}{\partial \theta} = \frac{\partial \tilde{L}_\phi}{\partial \phi} = 0, \quad \frac{\partial \tilde{L}_\theta}{\partial \phi} + \frac{\partial \tilde{L}_\phi}{\partial \theta} = 4\sigma\alpha_0 \sin \phi \neq 0.$$

Thus the only stable equilibrium is E 2₋, and if $B\sigma$ exceeds the critical value for it to exist, ($[2(1+\alpha_0)]^{-1}$ for $\alpha_0 < \frac{1}{3}$, and $[32\alpha_0(1-\alpha_0)]^{-\frac{1}{2}}$ for $\alpha_0 > \frac{1}{3}$), the cells must tumble. These results for non-zero α_0 confirm Kessler's view that, when the vorticity in the Poiseuille flow, evaluated at the cell's location, becomes too large, then there is no stable equilibrium configuration and the cell will tumble. It is intended to perform experiments with different types of cell in which the critical value of σ can be measured both as a test of the theory and as a means of measuring B .

It is interesting to note that the equilibrium E1 is unstable for non-zero α_0 (non-spherical cells) but becomes neutrally stable when $\alpha_0 = 0$; the corresponding equilibrium from §3.1 (with $\alpha_0 = 0$) is stable for non-zero ω'_3 but becomes neutrally stable when $\omega'_3 = 0$. To investigate the interaction between non-zero vertical relative vorticity ($\omega'_3 \neq 0$) and non-spherical geometry ($\alpha_0 \neq 0$), consider spiral (downwards) Couette flow in a vertical annulus of outer radius a_0 , in which (say)

$$U = 0; \quad V = -\Omega r + \Gamma/r; \quad W = A \ln(r/a_0),$$

where V is the swirl velocity and Ω, Γ, A are positive constants. Defining $\sigma = A/2r$, we again have (cf. (30))

$$\omega_2 = -2\sigma, \quad \epsilon_{13} = \sigma.$$

We also have $\epsilon_{12} = \frac{1}{2}r d/dr(V/r) = -\Gamma/r^2 = -e$ (say)

and a non-zero value of ω'_3 , since the angular velocity of the axes, Ω_{c3} , is V/r while $\omega_3 = 1/r \times d/dr(rV)$; thus, from (14)

$$\omega'_3 = dV/dr - V/r = -2e,$$

independent of the solid-body rotation Ω . Equations (19) and (20) now yield

$$\tilde{L}_\theta = -B^{-1} \sin \theta - 2\sigma \cos \phi (1 - \alpha_0 \cos 2\theta) - e\alpha_0 \sin 2\theta \sin 2\phi = 0,$$

$$\tilde{L}_\phi / \sin \theta = 2\sigma(1 - \alpha_0) \cos \theta \sin \phi - 2e \sin \theta (1 + \alpha_0 \cos 2\phi) = 0.$$

To examine the competing effects of non-sphericity ($\alpha_0 \neq 0$) and non-zero ω'_3 ($e \neq 0$) we restrict attention to values of α_0 and e/σ which are small and comparable in magnitude with each other. A little calculation then shows that, if $2B\sigma < 1$, there is a single, stable equilibrium with

$$\sin \theta \approx 2B\sigma (\cos \theta > 0), \quad \cos \phi \approx -1 (\phi \approx \pi);$$

this is no different from the case of Poiseuille flow without swirl. However, if $2B\sigma > 1$, there is again a single equilibrium, with

$$\cos \theta \approx 2Be(4B^2\sigma^2 - 1)^{-\frac{1}{2}}, \quad \cos \phi \approx -1/(2B\sigma),$$

which is stable (according to the second inequality in (23a)) if

$$2Be > \alpha_0(4B^2\sigma^2 - 1) \tag{37}$$

but unstable otherwise. It would be most interesting to test the extent to which the focusing properties of algae are in fact affected by non-solid-body swirl.

The transition from spin to no spin may also occur in vertical Poiseuille flow focusing. Because $\sigma \propto r$ (equation (30)), the cell swims from regions of high (low) ω to regions of low (high) ω in a downward (upward) flow. It should be possible to observe microscopically the general region where the cells acquire an extra angular velocity, Ω' . Such a measurement would be useful for determining the gyrotactic orientation constant B . It is also possible, in principle, to observe the transition from tumbling to autorotation when $2B\sigma > 1$ and ω'_3 (i.e. e) is increased above the value given by (37). Such an observation would be a useful confirmation of the theory.

(b) Conical sink flow

This flow, depicted in figure 4, is included as an example with rate of strain but no vorticity. It is easily realizable, and indeed has particular relevance to gyrotactic focusing experiments, because suspensions of algae are fed into the pipe through a conical inlet region. Here

$$U = -Qr/R^2, \quad W = -Qz/R^2, \quad \omega = 0,$$

$$e_{11} = -e_{33} = Q(r^2 - z^2)/R^4; \quad e_{22} = -Q/R^2; \quad e_{13} = 2Qrz/R^4, \quad (38)$$

where Q is a constant flow rate and $R^2 = r^2 + z^2$. Substitution into (20) shows that $\tilde{L}_\phi/\sin\theta = 0$ if either $\sin\phi = 0$ or

$$r \sin\theta \cos\phi = -z \cos\theta. \quad (39)$$

The latter, substituted into (19), gives $\sin\theta = 0$, so that it does not correspond to an equilibrium unless $z = 0$, a neutrally stable degenerate case which we ignore.

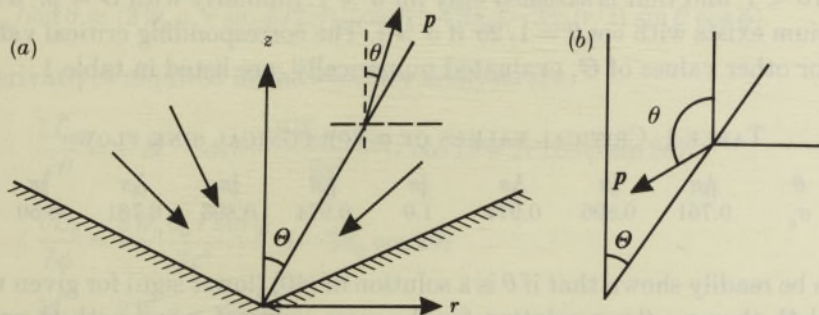


FIGURE 4. Conical sink flow: local equilibria (a) with $\phi = 0$ and $\theta < \Theta$, which exists and is stable for all σ ; (b) with $\phi = \pi$ and $\theta > \frac{1}{2}\pi$ which exists and is stable for $\sigma > \sigma_c$. (See text for details.)

If $\sin\phi = 0$, then $\cos\phi = \pm 1$ ($\phi = 0$ or π), and (19) gives

$$\sin\theta = -\sigma \sin[2(\theta \mp \Theta)] \quad (40)$$

where $\sigma = 2BQ\alpha_0/R^2 > 0$ (a measure of the strength of the straining motion at the cell) and $\tan\Theta = r/z$ (figure 4a); we suppose that $\Theta \leq \frac{1}{2}\pi$. The quantities needed for determining stability (when $\sin\phi = 0$) are

$$\partial\tilde{L}_\theta/\partial\theta = -B^{-1}\{\cos\theta + 2\sigma \cos[2(\theta \mp \Theta)]\}, \quad (41a)$$

$$\partial\tilde{L}_\phi/\partial\phi = \mp[(4\alpha_0 \sin\Theta \sin\theta)/R^2] \cos(\theta \mp \Theta), \quad (41b)$$

$$\partial\tilde{L}_\theta/\partial\phi = \partial\tilde{L}_\phi/\partial\theta = 0.$$

With the upper sign ($\phi = 0$), these equations show that a stable equilibrium configuration exists with $\theta < \Theta$ (figure 4a) for all values of σ ; cells will swim away from the sink ($\theta < \frac{1}{2}\pi$) and away from the axis ($\phi = 0$), but will move onto streamlines that are closer to the axis ($\theta < \Theta$). With the lower sign ($\phi = \pi$), (40) shows that

$$\frac{1}{2}\pi < \theta + \Theta < \pi \quad (42)$$

for an equilibrium to exist, and in that case $\partial\tilde{L}_\phi/\partial\phi < 0$ from (41b); stability therefore requires

$$\cos\theta + 2\sigma \cos[2(\theta + \Theta)] > 0. \quad (43)$$

If $\sigma \gg 1$, (40) gives

$$\theta + \Theta \approx \frac{1}{2}\pi + \cos\Theta/2\sigma \quad \text{or} \quad \pi - \cos\Theta/2\sigma,$$

and the latter of these satisfies (43), giving a stable equilibrium. If $\sigma \ll 1$, on the other hand, (40) shows that $\sin\theta$ is small; this result is inconsistent with (42) and suggests that a second stable equilibrium exists (figure 4b) but only if σ is large enough, a conclusion which can be confirmed analytically for the special cases $\Theta = \frac{1}{4}\pi, \frac{1}{2}\pi$. For $\Theta = \frac{1}{4}\pi$, (40) with the lower sign can be solved to give

$$\sin\theta = [1 + \sqrt{(1 + 8\sigma^2)}]/4\sigma, \quad (44)$$

where the negative square root has been eliminated because $\sin\theta > 0$. The inequality (42) requires $\sin\theta > 1/\sqrt{2}$, which is satisfied for all $\sigma > 0$, as is the stability requirement (43) if we choose the solution of (44) with $\theta > \frac{1}{2}\pi$, but we also need $\sin\theta < 1$, and that is satisfied only for $\sigma > 1$. Similarly with $\Theta = \frac{1}{2}\pi$, a stable equilibrium exists with $\cos\theta = 1/2\sigma$ if $\sigma > \frac{1}{2}$. The corresponding critical values of σ (σ_c) for other values of Θ , evaluated numerically, are listed in table 1.

TABLE 1. CRITICAL VALUES OF σ FOR CONICAL SINK FLOW

θ	$\frac{1}{16}\pi$	$\frac{1}{8}\pi$	$\frac{3}{16}\pi$	$\frac{1}{4}\pi$	$\frac{5}{16}\pi$	$\frac{3}{8}\pi$	$\frac{7}{16}\pi$	$\frac{1}{2}\pi$
σ_c	0.761	0.896	0.974	1.0	0.974	0.896	0.761	0.50

It can be readily shown that if θ is a solution of (40) (lower sign) for given values of σ and Θ , then $\pi - \theta$ is a solution for the same value of σ and with Θ replaced by $\frac{1}{2}\pi - \Theta$; the value of the left-hand side of (43) is unchanged. This explains the symmetry to be seen in table 1.

The existence of two possible stable equilibria for sufficiently large σ raises the interesting prospect of a group of swimming algae separating themselves into two populations, one swimming up relative to the flow and one swimming down. An experimental test of this prediction is under construction.

(c) Wake of a falling sphere

There are certain freshwater Crustacea (cladocerans), much larger than algae (which they eat) but still moving at small values of the Reynolds number, whose lifestyle includes intermittent up and down movement in their aqueous environment, presumably to increase the amount of food accessible to them (M. Gophen, personal communication). They are observed to fall under gravity from one level to a deeper one, and then to swim up again to approximately the original level. If the water were still, and during the falling phase swimming algae were focused into the animal's wake, it could make their subsequent capture energetically less costly (figure 5). Although such a mechanism is entirely conjectural, it is of interest to check whether algae will be focused into the wake.

Consider a sphere of radius a_0 falling at low Reynolds number with terminal

velocity W_0 . The radial and axial velocity components (calculated from the Stokes formulae usually given in spherical polars) are

$$\left. \begin{aligned} U &= -\frac{3W_0}{4R^2} \left(\frac{a_0}{R} - \frac{a_0^3}{R^3} \right); \\ W &= -\frac{3W_0}{4} \left(\frac{a_0}{R} \frac{r^2 + 2z^2}{R^2} + \frac{a_0^3}{R^3} \frac{r^2 - 2z^2}{R^2} \right), \end{aligned} \right\} \quad (45)$$

where $R^2 = r^2 + z^2$; ω and e_{ij} can be calculated from (28) and (29). Rather than investigate all possible positions of the cell, we shall concentrate on the region near the axis of symmetry, behind the sphere and relatively far from it; i.e. we assume $z > 0$, $r/z \ll 1$, $a/z \ll 1$. This means that only the first, Stokeslet, terms in (45) contribute to the leading terms in \tilde{L}_θ and $\tilde{L}_\phi/\sin\theta$, which, from (19) and (20), become:

$$\tilde{L}_\theta \approx -B^{-1} \sin\theta - (3W_0 a_0 / 4z^3) \{3\alpha_0 z \sin 2\theta + 2r \cos\phi (1 - 3\alpha_0 \cos 2\theta)\} \quad (46a)$$

$$\tilde{L}_\phi/\sin\theta \approx (3W_0 a_0 r \sin\phi / 2z^3) \{\cos\theta (1 - 3\alpha_0) - 3\alpha_0 (r/z) \sin\theta \cos\phi\}. \quad (46b)$$

The derivatives required in the stability analysis are:

$$\frac{\partial \tilde{L}_\theta}{\partial \theta} = -B^{-1} \cos\theta - \frac{9W_0 a_0 \alpha_0}{2z^3} \{z \cos 2\theta + 2r \cos\phi \sin 2\theta\} \quad (47a)$$

$$\frac{\partial \tilde{L}_\theta}{\partial \phi} = \frac{3W_0 a_0 r \sin\phi}{2z^3} \{1 - 3\alpha_0 \cos 2\theta\} \quad (47b)$$

$$\frac{\partial \tilde{L}_\phi}{\partial \theta} = \frac{3W_0 a_0 r \sin\phi}{2z^3} \{(1 - 3\alpha_0) \cos 2\theta - 3\alpha_0 (r/z) \cos\phi \sin 2\theta\} \quad (47c)$$

$$\frac{\partial \tilde{L}_\phi}{\partial \phi} = \frac{3W_0 a_0 r \sin\theta}{2z^3} \{(1 - 3\alpha_0) \cos\theta \cos\phi - 3\alpha_0 (r/z) \sin\theta \cos 2\phi\}. \quad (47d)$$

This system seems to present several possible equilibria, which we enumerate as follows, recalling that $r/z \ll 1$.

$$E1. \quad \sin\phi = 0 \quad \text{and} \quad \cos\theta = -2z^2/9BW_0 a_0 \alpha_0.$$

This requires that the magnitude of the last expression be less than 1. On the other hand the stability requirement $\partial \tilde{L}_\theta / \partial \theta < 0$ requires that the same quantity should exceed 1, so this equilibrium is never stable.

$$E2. \quad \sin\phi = 0 \quad \text{and} \quad \sin\theta = 0(r/z).$$

If we set $\sin\theta = \gamma r/z$ in $\tilde{L}_\theta = 0$ ($\gamma = 0(1)$ and $\gamma > 0$), so that $\cos\theta$ may be close to ± 1 , we obtain

$$\gamma [1 + (9BW_0 a_0 \alpha_0 \cos\theta / 2z^2)] = -3BW_0 a_0 (1 - 3\alpha_0) \cos\phi / 2z^2. \quad (48)$$

Thus if the square bracket is positive, $\gamma > 0$ if $(1 - 3\alpha_0) \cos\phi < 0$, and vice versa; moreover the equilibrium is stable if both $(1 - 3\alpha_0) \cos\theta \cos\phi < 0$ and

$\cos \theta + 9BW_0 a_0 \alpha_0 / z^2 > 0$. Thus stable equilibria occur (i) for $\cos \theta \approx +1$ (small θ , i.e. the cell is pointing almost vertically up) and $\phi = 0$ or π according as $\alpha_0 \gtrless \frac{1}{3}$ (this exists for all B), and (ii) for $\cos \theta \approx -1$ (θ close to π) and $\phi = \pi$ or 0 according as $\alpha_0 \gtrless \frac{1}{3}$, but this one only exists if

$$BW_0 a_0 \alpha_0 / z^2 > \frac{2}{9}. \quad (49)$$

Case (i) is particularly interesting, because it implies that cells will be focused *inwards* ($\phi = \pi$) if $\alpha_0 < \frac{1}{3}$, but *outwards* ($\phi = 0$) if $\alpha_0 > \frac{1}{3}$: long, thin algae can escape the attentions of the predatory cladoceran but nearly spherical ones cannot! Note that the opposite is true for case (ii), but since this requires (49) to be satisfied it is less generally relevant.

$$\text{E3. } \sin \phi \neq 0 \text{ but } \cos \theta(1-3\alpha_0) = 3\alpha_0 \frac{r}{z} \sin \theta \cos \phi, \text{ from (46b).}$$

Thus we try $\theta = \frac{1}{2}\pi - \theta'$, for $\theta' \ll 1$, and obtain

$$\theta' = -\frac{2\alpha_0 z^2}{BW_0 a_0}, \quad \cos \phi = -\frac{2(1-3\alpha_0)z^3}{3BW_0 a_0 r}. \quad (50)$$

The condition $|\cos \phi| < 1$ is very restrictive, since $r/z \ll 1$, and in any case the equilibrium is unstable because $\partial \tilde{L}_\phi / \partial \phi > 0$.

The above analysis suggests that all but long, thin algae will be focused into the wake of a falling sphere. If the sphere were a cladoceran, it could then swim up and consume them unless the fact of its upward swimming caused them to be oriented so that they could swim away from the axis of symmetry. Now the far-field, Stokeslet terms in the velocity components (45), which are responsible for the inward focusing demonstrated above, are completely determined by the force exerted on the fluid by the body (Batchelor (1967) p. 240). This force is exactly the same, equal to the reduced weight of the body and directed downwards, whether the body is falling at its terminal speed W_0 , hovering at rest or swimming upwards at an arbitrary speed. Thus the inward focusing of the algae will continue

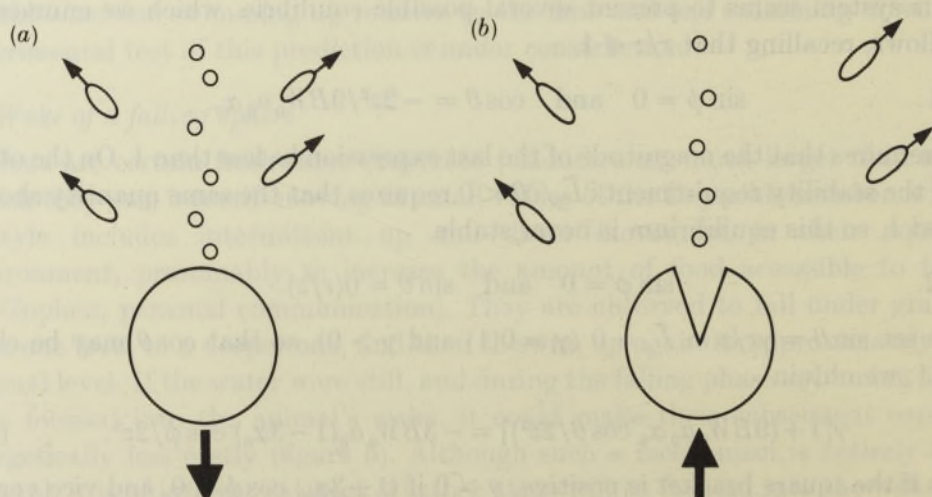


FIGURE 5. (a) Focusing into or out of the far wake of a falling sphere;
(b) focusing unchanged if the 'sphere' swims upwards.

while the cladoceran swims upwards, and their capture is rendered more probable (although the details of capture would depend on the *near* flow field: cf. Childress *et al.* 1987). This is a rather interesting, and somewhat surprising, prediction.

We might note further what happens to algae originally *below* the cladoceran as it falls. The same analysis holds, except that z is taken to be negative. The conclusions are very similar to the above except that it is the long, thin algae ($\alpha_0 > \frac{1}{3}$) that are focused *in* and the more spherical ones that are focused *out*. Thus the long, thin ones do not escape after all, because they can be consumed while the animal is falling down.

The analysis of this section would also be applicable to focusing behind (or in front of) a falling drop of liquid whose density exceeds that of the surrounding medium. This may be particularly relevant to the ‘blips’ formed when a focused beam of algae becomes unstable, for example when the surrounding flow is not vigorous enough (Kessler 1986*b*).

3.3. Two-dimensional motion in a vertical plane

(a) Pure straining motion

This two-dimensional stagnation point flow is relatively simple to realize experimentally using four rollers (Taylor 1934). It is depicted in figure 6, where the axis along which the flow is inwards makes an angle ψ with the vertical; without loss of generality $0 \leq \psi \leq \frac{1}{2}\pi$. The flow has zero vorticity and uniform strain rate E , so that the non-zero components of the rate-of-strain tensor are

$$e_{11} = -e_{33} = E \cos 2\psi, \quad e_{13} = -E \sin 2\psi. \quad (51)$$

Thus equations (19) and (20) give

$$\tilde{L}_\theta = -B^{-1} \sin \theta + \alpha_0 E \{ \cos 2\psi \sin 2\theta (1 + \cos^2 \phi) - 2 \sin 2\psi \cos 2\theta \cos \phi \} \quad (52a)$$

$$\tilde{L}_\phi / \sin \theta = \alpha_0 E \{ -\cos 2\psi \sin \theta \sin 2\phi + 2 \sin 2\psi \cos \theta \sin \phi \}, \quad (52b)$$

and the derivatives required for assessing stability can easily be derived from these equations.

Two distinct classes of equilibria appear to be possible in this case, as follows:

$$E1. \quad \phi = 0 \text{ or } \pi \quad (\cos \phi = \pm 1) \quad \text{and} \quad \sin \theta = \sigma \sin [2(\theta \mp \psi)] \quad (53)$$

$$\text{where} \quad \sigma = 2B\alpha_0 E; \quad (54)$$

stability requires that both

$$\sin (\theta \mp 2\psi) > 0 \quad (55)$$

$$\text{and} \quad -\cos \theta + 2\sigma \cos [2(\theta \mp \psi)] < 0. \quad (56)$$

$$E2. \quad \cos \theta = (1/\sigma) \cos 2\psi \quad \text{and} \quad \sin \theta \cos \phi = (1/\sigma) \sin 2\psi, \quad (57)$$

which can exist only if $\sigma > \max(|\cos 2\psi|, \sin 2\psi)$; stability requires $\sin 4\psi < 0$ (i.e. $\psi > \frac{1}{4}\pi$) together with both

$$A \equiv 1 + 2 \sin^2 2\psi + 2 \cos^2 2\psi \cos^2 \phi - \sigma^2 (1 + \cos^2 \phi) > 0 \\ \text{and} \quad 2 \cos^2 2\psi A - \sigma^4 \cos^2 \phi > 0. \quad (58)$$

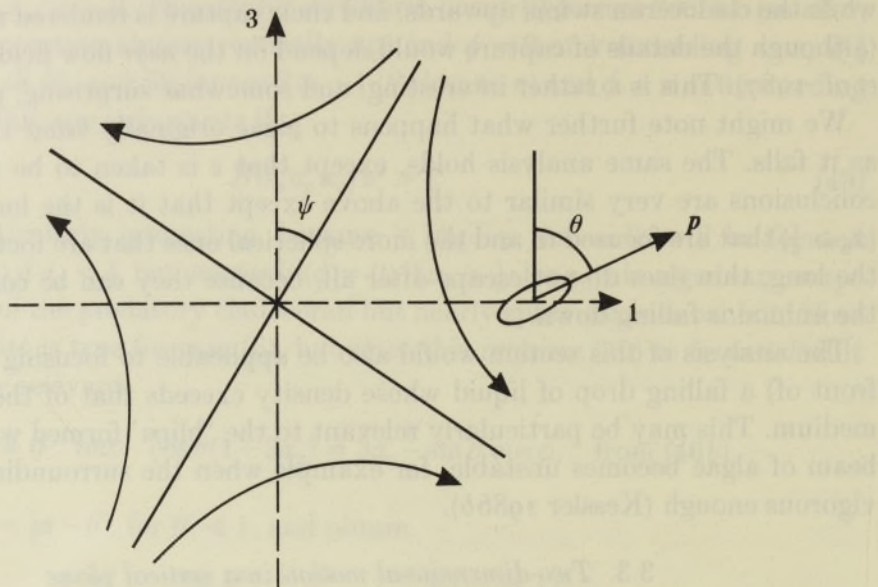


FIGURE 6. Stagnation-point flow in a vertical plane.

For general values of ψ and σ these equilibria have to be examined numerically, but analytical conclusions can be drawn in particular cases or limits, listed below.

(i) $\psi = 0$. E_1 gives stable equilibria for both $\phi = 0$ and $\phi = \pi$ at which $\cos \theta = \frac{1}{2}\sigma$ if $\sigma > \frac{1}{2}$, and E_1 or E_2 gives a stable equilibrium with $\theta = 0$ if $\sigma < \frac{1}{2}$ (in this case the stability is assessed by means of (23b)). There is no other stable equilibrium E_2 .

(ii) $\psi = \frac{1}{2}\pi$. E_1 does not give a stable equilibrium with $\sin \theta \neq 0$, but there is a stable equilibrium with $\theta = 0$ (nose-up) for all values of σ ; moreover, $\theta = \pi$ (nose-down) also gives a stable equilibrium for $\sigma > 1$ (these are again assessed by means of (23b)). E_2 gives another equilibrium with $\cos \phi = 0$ and $\cos \theta = -1/\sigma$, for $\sigma > 1$, but this is unstable from (58).

(iii) $\psi = \frac{1}{4}\pi$. The only equilibrium given by E_2 has $\theta = \frac{1}{2}\pi$ and $\cos \phi = 1/\sigma$ ($\sigma > 1$), but this is unstable from the second inequality in (23a) or (58). E_1 , however, gives a stable equilibrium with $\phi = \pi$, $\sin \theta = [-1 + \sqrt{(1+8\sigma^2)}]/4\sigma$ and $\cos \theta > 0$ (nose-up) for all positive values of σ , and another stable equilibrium with $\sigma = 0$, $\sin \theta = [-1 + \sqrt{(1+8\sigma^2)}]/4\sigma$ and $\cos \theta < 0$ (nose-down) for $\sigma > 1$.

(iv) $\sigma = 1$. In this case E_1 gives four different equilibria: there is one at $\phi = \pi$, $\theta = \frac{1}{3}(\pi - 2\psi)$, which is stable for all ψ (in the range $0 < \psi < \frac{1}{2}\pi$); one at $\phi = 0$, $\theta = \frac{1}{3}(\pi + 2\psi)$, which is stable only if $\psi < \frac{1}{4}\pi$; one at $\phi = \pi$, $\theta = \pi - \frac{2}{3}\psi$, which is unstable; and one at $\phi = 0$, $\theta = 2\psi$ which is unstable for $\psi < \frac{1}{4}\pi$ and neutrally stable for $\psi > \frac{1}{4}\pi$ (since both sides of the second inequality (23a) are zero); this last is also the only equilibrium given by E_2 .

(v) $\sigma \ll 1$. There is no equilibrium given by E_2 , and one stable equilibrium given by E_1 , with $\phi = \pi$ and $\theta \approx \sigma \sin 2\psi$.

(vi) $\sigma \gg 1$. E_1 gives two stable equilibria for all ψ , one with $\phi = 0$, $\theta \approx \frac{1}{2}\pi + \psi - (\cos \psi / 2\sigma)$ and the other with $\phi = \pi$, $\theta \approx \frac{1}{2}\pi - \psi - (\cos \psi / 2\sigma)$. E_2 gives no stable equilibria, from (58).

The above analytical results have been supplemented by numerical calculations

for intermediate values of ψ or σ . A selection of the results is given in table 2; they can be summarized with the help of figure 7 as follows. For all values of ψ and σ there is a stable equilibrium given by E 1, with $\phi = \pi$ (swimming in towards a vertical axis through the stagnation point) and $0 \leq \theta \leq \frac{1}{2}\pi$. In fact, for a given ψ , θ increases from 0 to $\frac{1}{2}\pi - \psi$ as σ increases from 0 to ∞ . Again, for every ψ there is an equilibrium (E 1) with $\phi = 0$ (swimming out), but this exists and is stable only if σ exceeds a critical value that depends on ψ , σ_c say, when $\theta = \theta_c$; θ increases from θ_c to $\frac{1}{2}\pi + \psi$ as σ increases from σ_c to infinity.

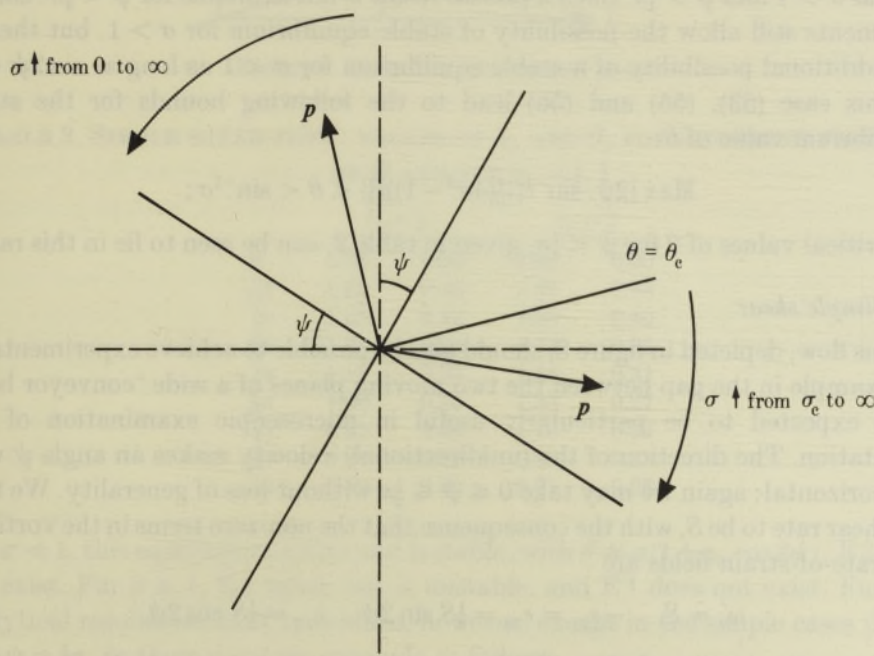


FIGURE 7. Local stable equilibrium orientations for stagnation-point flow, showing how p varies as σ varies.

TABLE 2. CRITICAL VALUES OF σ AND θ FOR EQUILIBRIUM OF
PURE STRAINING MOTION WITH $\phi = 0$

ψ	σ_c	θ_c
$\frac{1}{16}\pi$	0.77	0.26π
$\frac{1}{8}\pi$	0.90	0.35π
$\frac{3}{16}\pi$	0.98	0.44π
$\frac{1}{4}\pi$	1.0	$\frac{1}{2}\pi$
$\frac{5}{16}\pi$	1.0	$\frac{5}{8}\pi$
$\frac{3}{8}\pi$	1.0	$\frac{3}{4}\pi$
$\frac{7}{16}\pi$	1.0	$\frac{7}{8}\pi$

It will be seen from table 2 that $\sigma_c = 1.0$ and $\theta_c = 2\psi$ for all $\psi \geq \frac{1}{4}\pi$. This can be demonstrated simply from (53), (55) and (56), with the upper sign, as follows. Since $\sin \theta > 0$, (53) shows that $\sin(2\theta - 2\psi) > 0$, and hence that $\psi < \theta < \frac{1}{2}\pi + \psi$. Moreover (55) shows that $\sin(\theta - 2\psi) > 0$ for stability, and hence

$$2\psi < \theta < \frac{1}{2}\pi + \psi. \quad (59)$$

If $\sigma < 1$, (53) then shows that either $\frac{1}{2}\pi < 2\theta - 2\psi < \theta$ or $\theta < 2\theta - 2\psi < \frac{1}{2}\pi$; the former is inconsistent with (59) and the latter implies $2\psi < \theta < \frac{1}{2}\pi$, which is impossible if $\psi > \frac{1}{4}\pi$. Hence there is no stable equilibrium with $\phi = 0$ for $\psi > \frac{1}{4}\pi$ and $\sigma < 1$. If $\sigma > 1$, on the other hand, (53) shows that either $2\theta - 2\psi < \theta < \frac{1}{2}\pi$, which is inconsistent with (59), or $\frac{1}{2}\pi < \theta < 2\theta - 2\psi$, which is consistent. In this case, (56) shows that such an equilibrium will always be stable, since $\cos(2\theta - 2\psi) < \cos\theta < 0$ and hence $(-\cos\theta/\sigma) + 2\cos(2\theta - 2\psi) < (2 - 1/\sigma)\cos\theta < 0$ because $\sigma > 1$. Thus there is always a stable equilibrium with $2\psi < \theta < \pi$ as long as $\sigma > 1$ and $\psi > \frac{1}{4}\pi$. Such a precise result is not available for $\psi < \frac{1}{4}\pi$: similar arguments still allow the possibility of stable equilibrium for $\sigma > 1$, but there is the additional possibility of a stable equilibrium for $\sigma < 1$ as long as $\sin 2\psi < \sigma$. In this case (53), (55) and (56) lead to the following bounds for the stable equilibrium value of θ :

$$\text{Max} \{2\psi, \sin^{-1}[(\frac{1}{3}(4\sigma^2 - 1))^{\frac{1}{2}}]\} < \theta < \sin^{-1}\sigma;$$

the critical values of θ for $\psi < \frac{1}{4}\pi$, given in table 2, can be seen to lie in this range.

(b) Simple shear

This flow, depicted in figure 8, should also be possible to achieve experimentally, for example in the gap between the two moving planes of a wide ‘conveyor belt’. It is expected to be particularly useful in microscopic examination of cell orientation. The direction of the (unidirectional) velocity makes an angle ψ with the horizontal; again we may take $0 \leq \psi \leq \frac{1}{2}\pi$ without loss of generality. We take the shear rate to be S , with the consequence that the non-zero terms in the vorticity and rate-of-strain fields are

$$\omega'_2 = S, \quad -e_{11} = e_{33} = \frac{1}{2}S \sin 2\psi, \quad e_{13} = \frac{1}{2}S \cos 2\psi. \quad (60)$$

Thus equations (19) and (20) give

$$\begin{aligned} \tilde{L}_\theta = -B^{-1} \sin \theta + S \cos \phi + \frac{1}{2}\alpha_0 S \{ & -\sin 2\theta \sin 2\psi (1 + \cos^2 \phi) \\ & + 2 \cos 2\theta \cos 2\psi \cos \phi \}, \end{aligned} \quad (61a)$$

$$\tilde{L}_\phi / \sin \theta = S \sin \phi \{ -\cos \theta + \alpha_0 (\sin \theta \cos \phi \sin 2\psi - \cos \theta \cos 2\psi) \}, \quad (61b)$$

and the derivatives required in the stability analysis can readily be calculated.

Once more there appear to be two types of equilibrium, *E1* with $\sin \phi = 0$ and

$$\sin \theta = \pm \sigma \{ 1 + \alpha_0 \cos(2\theta \pm 2\psi) \} \quad (62)$$

(where now $\sigma = BS$, and the upper sign is taken for $\phi = 0$ and the lower for $\phi = \pi$), and *E2* with

$$\cos \theta = \frac{\alpha_0 \sin 2\psi}{\sigma(1 - \alpha_0^2)}, \quad \cos \phi = \frac{\cos \theta (1 + \alpha_0 \cos 2\psi)}{\alpha_0 \sin \theta \sin 2\psi}.$$

It can be seen that, since $\alpha_0 < 1$, the upper sign is needed in (62) to make $\sin \theta > 0$, so that all equilibria of type *E1* have $\phi = 0$; moreover, they require $\sigma < (1 - \alpha_0)^{-1}$ in order that $\sin \theta < 1$. The stability requirements for type *E1* are that both

$$\cos \theta + \alpha_0 \cos(\theta + 2\psi) > 0 \quad \text{and} \quad \cos \theta + 2\alpha_0 \sigma \sin(2\theta + 2\psi) > 0.$$

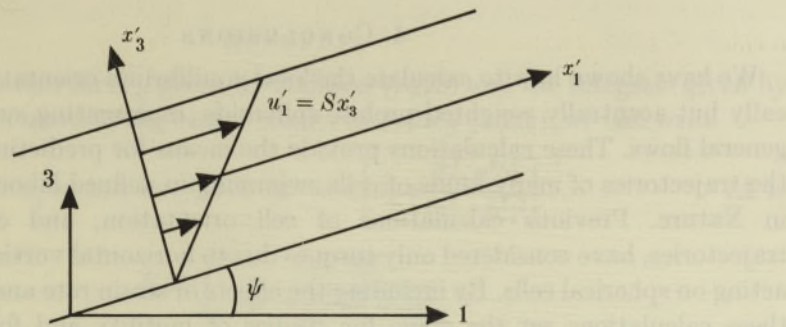


FIGURE 8. Shear flow in a vertical plane.

TABLE 3. SIMPLE SHEAR FLOW: VALUES OF σ_c AND θ_c FOR DIFFERENT VALUES OF ψ AND FOR $\alpha_0 = \frac{1}{4}, \frac{1}{2}$

	$\alpha_0 = \frac{1}{4}$		$\alpha_0 = \frac{1}{2}$	
	σ_c	θ_c	σ_c	θ_c
0	1.33	0.50	2.00	0.50
$\frac{1}{16}\pi$	1.32	0.46	1.97	0.45
$\frac{1}{8}\pi$	1.28	0.43	1.88	0.40
$\frac{3}{16}\pi$	1.21	0.40	1.73	0.35
$\frac{1}{4}\pi$	1.12	0.37	1.55	0.31
$\frac{5}{16}\pi$	1.03	0.35	1.33	0.27
$\frac{3}{8}\pi$	0.93	0.35	1.10	0.24
$\frac{7}{16}\pi$	0.84	0.37	0.88	0.23
$\frac{1}{2}\pi$	0.80	0.50	0.71	0.25

For $\sigma \ll 1$, this equilibrium exists and is stable, with $\theta \approx \sigma(1 + \alpha_0 \cos 2\psi)$; E2 does not exist. For $\sigma \gg 1$, E2 exists but is unstable, and E1 does not exist. Further analytical results are hard to achieve, however, except in the simple cases $\psi = 0$ and $\psi = \frac{1}{2}\pi$; in those cases we conclude as follows.

$\psi = 0$: here a stable equilibrium exists only if $\sigma < (1 - \alpha_0)^{-1}$, and has $\phi = 0$, $\cos \theta > 0$ (nose-up) and

$$\sin \theta = (1/4\alpha_0 \sigma) \{-1 + [1 + 8\alpha_0(1 + \alpha_0)\sigma^2]^{\frac{1}{2}}\}.$$

$\psi = \frac{1}{2}\pi$: Here again there is only one stable equilibrium possible, for which $\phi = 0$, $\cos \theta > 0$ and

$$\sin \theta = (1/4\alpha_0 \sigma) \{1 - [1 - 8\alpha_0(1 - \alpha_0)\sigma^2]^{\frac{1}{2}}\};$$

this exists and is stable if and only if

$$\sigma < (1 + \alpha_0)^{-1} \quad \text{for } \alpha_0 < \frac{1}{3}, \quad \text{and} \quad \sigma < [8\alpha_0(1 - \alpha_0)]^{-\frac{1}{2}} \quad \text{for } \alpha_0 > \frac{1}{3}.$$

Results for other values of ψ have been computed numerically, and confirm that there is a critical value of σ (say σ_c) above which no stable equilibrium occurs, and below which there is just the one stable equilibrium of type E1, with $\phi = 0$ and $0 < \theta < \theta_c$, where θ_c is the value of θ when $\sigma = \sigma_c$. The value of σ_c and θ_c for several values of ψ and for $\alpha_0 = 0.25$ and 0.5 are given in table 3; the only point to note is that θ_c has a minimum at a value of ψ somewhat below $\frac{1}{2}\pi$ (for $\alpha_0 = \frac{1}{4}$, the minimum of θ_c is 0.348π for $\psi = 0.36\pi$ when $\sigma_c = 0.95$; for $\alpha_0 = \frac{1}{2}$, the corresponding values are $\theta_c = 0.227\pi$, $\psi = 0.44\pi$, $\sigma_c = 0.87$).

4. CONCLUSIONS

We have shown how to calculate the local equilibrium orientation of symmetrically but acentrally weighted prolate spheroids, representing swimming cells, in general flows. These calculations provide the means for predicting and analysing the trajectories of many kinds of cells swimming in defined laboratory flows, and in Nature. Previous calculations of cell orientation, and of the resulting trajectories, have considered only torques due to horizontal vorticity and gravity, acting on spherical cells. By including the effects of strain rate and cell elongation, these calculations set the stage for studies of motility and for predictions of microorganism accumulation, separation, and interaction in a wide variety of flows. Furthermore, the formalism presented here is expected to permit measurements of orientation mechanisms under control of the cell in terms of equivalent physical torques. It is anticipated that such measurements will use fluid flow fields and gravity torques to balance stimulus-directed locomotion, such as phototaxis, and autorotation, which occurs in most swimming algae.

It should also be repeated that the developments have, for historical reasons, been referred to cells that are posteriorly weighted bodies of revolution and which propel themselves by anterior flagella. There is, however, no reason why cells with tail propulsion and/or anterior centre-of-gravity offset should not obey the same types of equation. The problem of more general cell shapes, e.g. triaxial spheroids, remains for the future, as does the problem of interaction of the flagella with the flow field.

This paper has illustrated the results by a number of different flow fields. Although these flows are fairly easy to realize experimentally, many of the predicted local equilibria may be hard to observe, because they do not lead to such a simple final state as a single, focused beam of cells. However, it should be possible to test the predictions experimentally in a variety of cases, with a variety of cells, and infer the value of a cell's 'gyrotactic orientation parameter', B . Our results may also be of interest in the analysis of stress systems and in the sedimentation of suspensions of non-spherical particles that experience a body couple of gravitational, magnetic or other origin (cf. Brenner 1970*b*). Perhaps the most interesting prediction for many of the flow configurations considered is the presence of critical phenomena. This is manifested by the existence of a critical value of the parameter measuring the strength of the flow that applies the viscous torque to a cell relative to the gravitational torque, measured by B^{-1} (e.g. the quantities σ_c of §§3.2*b* and 3.3*a, b*).

We are particularly grateful to N. A. Hill for his constructive criticisms of this work. Partial support by the National Science Foundation on grant no. INT 85-13696, and by the Science and Engineering Research Council, is gratefully acknowledged.

APPENDIX

From the equation for Y_{ij} given by Rallison (1978) and the integrals given by Batchelor (1970), quoting the earlier results of Jeffrey (1922), we can write

$$\alpha_{\parallel} = 4(J_1 + I_1/2)^{-1}, \quad \alpha_{\perp} = 4 \left[J_2 + \frac{2I_2 a^2 b^2}{(a^2 + b^2)^2} \right]^{-1}, \quad (\text{A } 1)$$

where

$$I_1 = \int_0^\infty \frac{2ab^4 d\lambda}{(a^2 + \lambda)^{\frac{1}{2}} (b^2 + \lambda)^3}$$

$$J_1 = \int_0^\infty \frac{ab^2 \lambda d\lambda}{(a^2 + \lambda)^{\frac{1}{2}} (b^2 + \lambda)^3}$$

$$I_2 = \int_0^\infty \frac{ab^2(a^2 + b^2) d\lambda}{(a^2 + \lambda)^{\frac{3}{2}} (b^2 + \lambda)^2}$$

$$J_2 = \int_0^\infty \frac{ab^2 \lambda d\lambda}{(a^2 + \lambda)^{\frac{3}{2}} (b^2 + \lambda)^2}.$$

The quantities defined by (A 1) are the dimensionless constants required in equation (6).

REFERENCES

- Batchelor, G. K. 1967 *An introduction to fluid dynamics*. Cambridge University Press.
 Batchelor, G. K. 1970 The stress system in a suspension of force-free particles. *J. Fluid Mech.* **41**, 545–570.
 Brenner, H. 1970a Rheology of two-phase systems. *A. Rev. Fluid Mech.* **2**, 137–176.
 Brenner, H. 1970b Rheology of a dilute suspension of dipolar spherical particles in an external field. *J. Colloid Interface Sci.* **32**, 141–158.
 Childress, S. 1981 *Mechanics of swimming and flying*. Cambridge University Press.
 Childress, S., Koehl, M. A. R. & Miksis, M. 1987 Scanning currents in Stokes flow and the efficient feeding of small organisms. *J. Fluid Mech.* **177**, 407–436.
 Childress, S., Levandowsky, M. & Spiegel, E. A. 1975 Pattern formation in a suspension of swimming micro-organisms. *J. Fluid Mech.* **69**, 591–613.
 Hall, W. F. & Busenberg, S. N. 1969 Viscosity of magnetic suspensions. *J. chem. Phys.* **11**, 137–144.
 Jeffrey, G. B. 1922 The motion of ellipsoidal particles immersed in a viscous fluid. *Proc. R. Soc. Lond. A* **102**, 161–179.
 Kessler, J. O. 1984 Gyrotactic buoyant convection and spontaneous pattern formation in algal cell cultures. In *Nonequilibrium cooperative phenomena in physics and related fields* (ed. M. G. Velarde), pp. 241–248. New York: Plenum Press.
 Kessler, J. O. 1985a Hydrodynamic focusing of motile algal cells. *Nature, Lond.* **313**, 218–220.
 Kessler, J. O. 1985b Cooperative and concentrative phenomena of swimming micro-organisms. *Contemp. Phys.* **26**, 147–166.
 Kessler, J. O. 1986a The external dynamics of swimming micro-organisms. In *Progress in phycological research* (ed. F. E. Round), vol. 4, pp. 257–307. Bristol: Biopress.
 Kessler, J. O. 1986b Individual and collective fluid dynamics of swimming cells. *J. Fluid Mech.* **173**, 191–205.
 Kessler, J. O. & Cann, J. P. 1987 Behaviour of ciliated protozoa in a vertical Poiseuille flow. (In preparation.)
 Levandowsky, M., Childress, S., Spiegel, E. A. & Hunter, S. H. 1975 A mathematical model of pattern formation by swimming micro-organisms. *J. Protozool.* **22**, 296–306.
 Nultsch, W. 1983 Photocontrol of movement of *Chlamydomonas*. In *The biology of photoreception* (ed. D. J. Cosens & D. Vince-Prue). *Symp. Soc. exp. Biol.* **36**, 521–539.

- Nultsch, W. & Hoff, E. 1973 Investigations on pattern formation in Euglenae. *Arch. Protistenk.* **115**, 336–352.
- Rallison, J. M. 1978 The effects of Brownian rotations in a dilute suspension of rigid particles of arbitrary shape. *J. Fluid Mech.* **84**, 237–263.
- Rüffer, U. & Nultsch, W. 1985 High speed cinematographic analysis of the movement of *Chlamydomonas*. *Cell Motility* **5**, 251–263.
- Taylor, G. I. 1934 The formation of emulsions in definable fields of flow. *Proc. R. Soc. Lond. A* **146**, 501–523.